ANTIOXIDANTS & REDOX SIGNALING
Volume 11, Number 5, 2009

DOI: 10.1089/ars.2008.2262

Forum Original Research Communication

Modulation of Redox Switches of Copper Chaperone Cox17 by Zn(II) Ions Determined by New ESI MS-Based Approach

Kairit Zovo and Peep Palumaa

Abstract

Cox17, a copper chaperone for cytochrome-c oxidase, contains six conserved Cys residues and exists in three oxidative states, linked with two thiol-based redox switches. The first switch leads to formation of two disulfides and occurs upon transport of Cox17 into mitochondrial intermembrane space (IMS). $Cox17_{2S\text{-}S}$ is retained in the IMS and is also a functional form of the protein, which can be further oxidized to $Cox17_{3S\text{-}S}$. According to the midpoint redox potential values, Cox17 can be partially oxidized in the cytosol, which might hinder its transport into IMS. We hypothesize that Zn(II) ions might protect cytosolic Cox17 from oxidation. In order to get quantitative information about the modulatory effect of Zn(II) ions on redox switches in Cox17, we have used ESI MS for determination of the midpoint potentials for redox couples of Cox17: $Cox17_{3S\text{-}S} \leftrightarrow Cox17_{2S\text{-}S}$ (E_{m1}) and $Cox17_{2S\text{-}S} \leftrightarrow Cox17_{0S\text{-}S}$ (E_{m2}) in the presence of Zn(II). 10 μM Zn(II) ions shift the E_{m2} by 21 mV and E_{m1} by 15 mV to more positive values. Apparent dissociation constants for Zn(II) complexes of $Cox17_{0S\text{-}S}$ and $Cox17_{2S\text{-}S}$, are 0.067 and 0.29 nM, respectively. The high affinity shows that metallation of $Cox17_{0S\text{-}S}$ by Zn(II) might be significant in cellular conditions, which might protect Cox17 from oxidation and enable its transport into IMS. *Antioxid. Redox Signal.* 11, 985–995.

Introduction

Cellular functioning relies on strict regulation of the redox environment in the cytosol as well as in different subcellular compartments. Research over the last decades has established that cellular redox potential is dynamic and fluctuates substantially during various fundamental cellular activities, such as cell proliferation, hormonal signaling, transcriptional regulation, apotosis, and others (for review, see ref. 16). It has also become evident that cellular redox environment is primarily affected by cellular oxidative metabolism, redox signaling, and oxidative stress (for review, see ref. 35).

Cellular redox potential is created and maintained mainly by a redox couple composed of a low molecular weight thiol compound—glutathione (GSH) and its oxidized form—GSSG, which total cellular concentration is in the range of 2–10 mM (22). There is a complex enzymatic system, composed of thioredoxins, glutaredoxins, thioredoxin reductases, glutaperoxidases, and other enzymes that maintain the ratio of GSH/GSSG in the physiological range. This enzymatic system is also coupled with other redox couples primarily NADPH/NADP (10). However, these couples are not in equilibrium and moreover, their potentials differ among different cellular compartments and are subjected to substantial changes during various cellular activities (22).

Currently it is known that intracellular proteins might often undergo transient oxidation in cellular conditions. Large-scale studies have identified an increasing number of intracellular proteins that contain conserved subsets of cysteines, which are sensitive to oxidation and function as redox switches (20). Functioning of these thiol-based redox switches relies on reversible oxidation of thiols to disulfides, their nitrosylation, glutathionylation, or oxidation to sulfenic acid, which affects a broad range of biologically important properties of proteins such as conformation, activity of enzymes, transporters, and receptors, protein–protein and protein–DNA interactions, as well as protein trafficking and degradation (20, 35).

The state of thiol switches depends primarily on the environmental redox potential and the presence of labile reactive oxygen (ROS) or nitrogen species (RNS). However, the real biological situation is even more complex, and functioning of thiol-based redox switches might also be affected by metal

Department of Gene Technology, Tallinn University of Technology, Tallinn, Estonia.

ions, primarily by Zn(II), that can bind to spatially adjacent thiolates, thus affecting redox properties and functioning of these proteins (21). Based on current knowledge, Zn(II) ions affect thiol-based redox switches in diverse proteins such as Tim10 (23), Cox17(40), Kv channel (36), Erv2 (37), and others. Taking into account the relatively high affinity of Zn(II) ions for thiolate ligands, we can suggest that a metal-dependent regulation of thiol-based redox switches might be a rather general phenomenon.

Metal ions should be most directly involved in the regulation of redox switches present in metal-binding proteins that do contain multiple Cys residues in their metal-binding sites. Such cellular proteins are first of all zinc finger proteins and copper chaperones, which are sensitive to oxidation and are known to contain biological redox switches (19, 24, 32, 40). Oxidation on zinc- and copper-binding proteins in biological system is a rather complex phenomenon as oxidation leads to their inactivation, and released metal ions, especially Zn(II), can initiate a variety of regulatory and signaling effects (24).

The effect of metal ions on redox switches should be reflected primarily in the intrinsic protein redox parameter called midpoint redox potential (E_m) determining at which environmental redox potential value redox switching occurs. Determination of E_m values relies on the detection of the equilibrium between oxidized and reduced forms of the protein at different environmental redox potential values, created by various redox buffer sytems (8). Usually redox buffers such as GSH/GSSG or DTT/oxidized DTT couples are used, and the redox potential values for different component ratios can be calculated by using the Nernst equation (8). The content of oxidized and reduced forms of the protein are usually determined by a variety of spectroscopic or bioanalytical methods from the mixture of protein redox forms or after trapping and separation of different redox states (4, 8, 25, 29). The presence of metal ions might exclude or complicate the application of many available techniques as metal ions affect the spectroscopic properties of proteins as well as interfere with chemical modification of Cys residues. Therefore, there is a need for direct and reliable methods for the determination of protein midpoint redox potentials in the presence of metal ions. Moreover, by using the GSH/GSSG redox buffers that mimic cellular redox conditions, there is also need for determination of protein–GSH adducts, which occur in mildly oxidizing conditions and have a biological role in protein redox regulation (7, 9). Coexisting redox and molecular forms of proteins can be unambiguously detected by mass spectrometry (MS). Importantly, high resolution MS instruments can determine mass with accuracy sufficient for direct monitoring of disulfide bond formation and enables the monitoring of redox equilibria without chemical modification of Cys residues, which might be incomplete and result in additional errors.

In the current work we elaborated high resolution ESI TOF MS methodology for direct determination of protein midpoint redox potential in the absence and the presence of metal ions using copper chaperone Cox17 as a model protein. We used the biological redox buffer GSH/GSSG, as well as DTT/oxi-oxidized DTT couple, for the creation of environmental redox potential. Cox17 (MW 7 kDa) functions as a copper chaperone for cytochrome-c oxidase (CCO) in eukaryotic cells (11, 34). The mammalian Cox17 contains six absolutely conserved Cys residues and can exist in three redox states corresponding to the fully reduced $Cox17_{0S\text{-}S}$, the partially oxidized $Cox17_{2S\text{-}S}$, and the fully oxidized $Cox17_{3S\text{-}S}$ protein (28). Redox reactions are important for targeting of Cox17 into IMS, where $Cox17_{0S\text{-}S}$ is oxidized to $Cox17_{2S\text{-}S}$ through a mechanism mediated by Mia40 proteins (5, 26). $Cox17_{2S\text{-}S}$ is also a functional form of Cox17; it is responsible for the metallation of another copper chaperone Sco1 (3). Recent data indicate that $Cu_1Cox17_{2S\text{-}S}$ might also transfer metals to Sco1 protein, where two metal-binding Cys residues are oxidized to disulfide, demonstrating that metal transfer might be coupled to electron transfer and highlighting the importance of redox reactions in functioning of Cox17 (1).

The midpoint redox potentials between two redox pairs of Cox17—$Cox17_{0S\text{-}S} \leftrightarrow Cox17_{2S\text{-}S}$ and $Cox17_{2S\text{-}S} \leftrightarrow Cox17_{3S\text{-}S}$—have been recently determined by using the alkylation of free SH groups of Cox17 with iodoalkylamide (40). According to these values Cox17 should get partially oxidized in the cellular cytosol (14, 40). This is unfavorable as only the fully reduced proteins can be transported into IMS through the mitochondrial outer membrane pores (5, 26). In the cellular cytosol, the fully reduced Cox17 might be metallated with Zn(II) ions, which might protect $Cox17_{0S\text{-}S}$ from oxidation in the cyosol (40), $Cox17_{2S\text{-}S}$ might also be further oxidized to $Cox17_{3S\text{-}S}$ by oxidative stimuli in IMS, leading to its inactivation and Zn(II) ions might protect also $Cox17_{2S\text{-}S}$ from oxidation. The effect of metal ions on midpoint redox potentials of Cox17 are unknown; however, knowing the effect of metal ions on the redox equilibria of Cox17 is crucial for better understanding the mechanisms of Cox17 transport into IMS, as well as its functioning in metallation of Sco1 and CCO.

The effect of Zn(II) ions on redox switches in Cox17 determined by novel ESI MS-based method indicate that Zn(II) ions shift both midpoint redox potentials of Cox17 to more positive values in a concentration dependent manner, protecting Cox17 from oxidation. We also determined Zn(II) binding affinity for the fully reduced and the partially reduced Cox17 forms. The observed affinity suggests that metallation of Cox17 by Zn(II) might occur in cellular conditions. Biological implications connected with regulation of Cox17 redox switches by Zn(II) ions are discussed.

Materials and Methods

Materials

Recombinant human apo-$Cox17_{3S\text{-}S}$ was expressed and purified as described in (39). Oxidized DTT was synthesized from reduced DTT according to the protocol described in (6). Tris base and HEPES, both Ultrapure, MB Grade, were purchased from USB Corporation (Cleveland, OH), other reagents of analytical grade were from Sigma-Aldrich (St. Louis, MO).

Kinetics of $Cox17_{3S\text{-}S}$ reduction with GSH and DTT followed by ESI MS

Lyophilized $Cox17_{3S\text{-}S}$ was dissolved in 20 m*M* ammonium acetate, pH 7.5, at 150 μM concentration, and this stock solution was used for the future experiments. 5 μM $Cox17_{3S\text{-}S}$ was incubated at 40°C in argon-saturated 20 m*M* ammonium acetate buffer, pH 7.5, containing different concentrations of GSH (1 or 2 m*M*) or 5 m*M* DTT as reducing agents. For the measurement of kinetics of $Cox17_{3S\text{-}S}$ reduction, 60 μl of aliquots from the reaction mixture were taken at various time

points and infused directly by a syringe pump at 10 μl/min into a QSTAR Elite ESI-Q-TOF mass spectrometer (Applied Biosystems, Foster City, CA). Mass spectra were recorded in the positive mode during 3–4 min in the region from 300 to 1,500 Da. Operating conditions were as follows: capillary exit voltage 5.5 kV; source gas 45 l/min; curtain gas 20 l/min; declustering potential 60 V; focusing potential 320 V; detector voltage 2,300 V. The obtained spectra were deconvoluted by program Bioanalyst 2.0 from Applied Biosystems. Kinetics of $Cox17_{3S\text{-}S}$ reduction was followed by increase of the average molecular weight of Cox17, and the kinetic curve was fitted by using the equation of first- order kinetics. For studies of the effect of millimolar Zn(II) ions on reduction of $Cox17_{3S\text{-}S}$ by 2 m*M* GSH, 5 μ*M* $Cox17_{3S\text{-}S}$ was incubated in argon-saturated 20 m*M* ammonium acetate buffer, pH 7.5, containing different concentrations of Zn(II) ions (1, 5, 10, and 50 m*M*) at 40°C. At various time points 100 μl aliquots from the reaction mixture were desalted and acidified using a HiTrap™ Desalting (5 ml) column (Amersham Biosciences, Uppsala, Sweden) equilibrated with 0.1% formic acid, pH 2.85. Mass spectra from the obtained sample were recorded as described above.

Determination of the midpoint redox potential for Cox17 pairs by ESI MS

For the determination of the midpoint redox potential for Cox17 redox pairs, the fully oxidized $Cox17_{3S\text{-}S}$ (5 μ*M*) was incubated in various GSH- or DTT-based redox buffers at 40°C for 3 h, which was sufficient to reach the redox equilibrium between the protein forms. Two GSH buffers with different total concentration of GSH were used: [GSH] + 2 [GSSG] = 5 m*M*, and [GSH] + [GSSG] = 1 m*M*, for method evaluation as protein midpoint redox potential value in different buffers should be similar. For the measurement of equilibrium state in GSH-based redox buffers, 100 μl of the reaction mixture were desalted and acidified using a HiTrap™ Desalting (5 ml) column (Amersham Biosciences) equilibrated with 0.1% formic acid, pH 2.85. Acidification was used to avoid the reoxidation of reduced Cox17 forms. The obtained samples were infused by a syringe pump at 10 μl/min into QSTAR Elite ESI-Q-TOF mass spectrometer and ESI MS mass spectra were recorded during 3–5 min as described above. The obtained spectra were analyzed by program Bioanalyst 2.0 and average molecular weight of Cox17, reflecting the ratio of $Cox17_{2S\text{-}S}$ and $Cox17_{3S\text{-}S}$ forms in the sample was determined. The fractional content of $Cox17_{2S\text{-}S}$ (y) was determined by dividing the mass increment (average molecular weight of Cox17 minus molecular weight of $Cox17_{3S\text{-}S}$) by 2 (maximal mass increment in case of reduction of S–S bond). The fractional content of $Cox17_{2S\text{-}S}$-GSH and $Cox17_{2S\text{-}S}$-$(GSH)_2$ adducts were estimated by dividing the sum of peak areas of Cox17 adducts by summarized peak areas of all Cox17 forms.

The equilibrium ratios of Cox17 redox forms in DTT-based redox buffers were determined after 3 h incubation of $Cox17_{3S\text{-}S}$ (5 μ*M*) at 40°C in DTT/DTTox redox buffers ([DTT] + [DTTox] = 5 m*M*) by ESI-MS. The studies were conducted as described above with the only exception that before MS measurements the reaction mixtures were diluted fivefold in 0.1% formic acid, pH 2.85. The fractional content of $Cox17_{0S\text{-}S}$ was determined by dividing the mass increment (average molecular weight of Cox17 minus molecular weight of $Cox17_{2S\text{-}S}$) by 4 (maximal mass increment in case of reduction of two S–S bonds).

Redox potential of redox buffers has been adjusted in a large range by varying the ratio of reduced and oxidized forms of GSH and DTT and corresponding redox potentials have been calculated from the following Nernst equations:

$$E' = E'_0(\mathrm{GSH}) - (\mathrm{RT}/\mathrm{nF}) \ln \frac{[\mathrm{GSH}^2]}{[\mathrm{GSSG}]} \quad (1)$$

$$E' = E'_0(\mathrm{DTT}) - (\mathrm{RT}/\mathrm{nF}) \ln \frac{[\mathrm{DTT}]}{[\mathrm{DTTox}]} \quad (2)$$

where $E_0'(\mathrm{GSH}) = -0.24$ V (pH 7.0 and 25°C) (31), $E_0'(\mathrm{DTT}) = -0.323$ V (pH 7.0 and 30°C) (33), R is the gas constant ($8.315\ \mathrm{JK^{-1}mol^{-1}}$), n is the number of electrons transferred in the reaction, and F is the Faraday constant (9.6485×10^4 C $\mathrm{mol^{-1}}$). The E_0'(GSH) and E_0'(DTT) values have been recalculated for 40°C using the equations (1) and (2), and for pH 7.5 using the following equation:

$$E_{\mathrm{pH}} = E'_0 + (\mathrm{pH} - \mathrm{pH}_0) \times (\Delta E/\Delta \mathrm{pH}) \quad (3)$$

where $\Delta E/\Delta$pH is the change in E if the pH is increased by 1 unit equal to 60.1 mV (14).

Determination of Zn(II) effect on midpoint redox potential of $Cox17_{3S\text{-}S}$ / $Cox17_{2S\text{-}S}$ couple

For the estimation of the effect of Zn(II) ions on $Cox17_{3S\text{-}S}$/$Cox17_{2S\text{-}S}$ equilibrium, the midpoint redox potentials were determined in the presence of 10 and 50 μ*M* Zn(II) acetate in GSH- based redox buffers. The midpoint redox potential of $Cox17_{3S\text{-}S} \leftrightarrow Cox17_{2S\text{-}S}$ were determined by fitting the fractional content of $Cox17_{2S\text{-}S}$ to environmental redox potential E_h using the following equation (15):

$$y = y_0 + \frac{A}{1 + e^{(x_0 - x)/b}} \quad (4)$$

where y = fractional content of $Cox17_{2S\text{-}S}$; x = environmental redox potential (E_h); y_0, A, b = constants; x_0 = midpoint redox potential (E_m). Data fittings were performed by using the following values for constants $y_0 = 0$ (initial fractional content of $Cox17_{2S\text{-}S}$), A = 1 (final fractional content of $Cox17_{2S\text{-}S}$), b = 10 (1 m*M* GSH/GSSG buffer) or 12 (5 m*M* GSH/GSSG buffer) by program Origin 6.1 (Originlab Corp. Northampton, MA). Changing the parameter b did not change the obtained value for midpoint redox potential but improved the quality of the fit.

Determination of Zn(II) effect on midpoint redox potential of $Cox17_{2S\text{-}S}$ / $Cox17_{0S\text{-}S}$ pair

For the estimation of the effect of Zn(II) ions on the $Cox17_{2S\text{-}S}$/$Cox17_{0S\text{-}S}$ pair, the midpoint redox potentials were determined in the presence of 10 μ*M* Zn(II) acetate in the DTT-based redox buffer. Midpoint redox potential of $Cox17_{2S\text{-}S} \leftrightarrow Cox17_{0S\text{-}S}$ pair was determined by fitting the dependence of fractional content of $Cox17_{0S\text{-}S}$ on environmental redox potential E_h with equation (4) by using values $y_0 = 0$, A = 1, b = 10 as described above.

Determination of Zn(II)-binding affinity for Cox17 forms

For determination of Zn(II) binding affinity of $Cox17_{2S\text{-}S}$ and $Cox17_{0S\text{-}S,}$ we accommodated an ESI-MS based approach previously elaborated for determination of Cu(I) binding affinities (28). For this purpose, increasing concentrations of DTT (or GSH) were added to the metallated protein samples, the mixture was incubated for 2 min and analyzed for coexisting metallated and apo- form of the proteins by ESI MS. The added metal chelator (DTT or GSH) competes with the protein for Zn(II) ions and shifts the metallation equilibrium back to the apo-forms. In a standard experiment, 5 μM samples of $Cox17_{2S\text{-}S}$ or $Cox17_{0S\text{-}S}$ Zn(II) complexes in 20 mM ammonium acetate pH 7.5 containing various concentrations of DTT or GSH were injected into the electrospray ion source of QSTAR Elite ESI-Q-TOF MS instrument and the mass spectra were recorded as described above.

Results

Kinetics of $Cox17_{3S\text{-}S}$ reduction with GSH and DTT

The acquired ESI mass spectra of Cox17 displayed three main peaks with charges +5, +6, and +7, whereas in the presence of GSH two additional peaks corresponding to $Cox17_{2S\text{-}S}$-GSH and $Cox17_{2S\text{-}S}$-$(GSH)_2$ adducts were also detected. Individual charge state peaks displayed almost baseline-resolved isotopic resolution (Fig. 1), which allowed correct determination of average molecular weight of protein taking into account charge state distribution as well as isotopic resolution. By incubation of $Cox17_{3S\text{-}S}$ with GSH, an increase of the average molecular weight of Cox17 by approximately 2 Da was observed (Fig. 2A),which reflects the reduction of one disulfide bond. Reduction of $Cox17_{3S\text{-}S}$ with 1 and 2 mM GSH occurs with a half-life of ~43 min and consequently to reach the equilibrium samples have to be incubated for 3 h.

It is known from previous studies that the more powerful reducing reagent DTT reduces $Cox17_{3S\text{-}S}$ to $Cox17_{2S\text{-}S}$ almost instantly, and moreover, it could be also used for further reduction of two remaining disulfides in $Cox17_{2S\text{-}S}$ (28, 39). The results obtained in the current study indicate that 5 mM DTT leads to almost instant increase of Cox17 average molecular weight by 2 Da, which is followed by further slower increase up to 6 Da (Fig. 2), accompanied with the shift in charge- state distribution from +6 and +7, forms to 6 charge states with charges between +5 and +10, characteristic for the fully reduced Cox17 (28). The reduction of two disulfides in $Cox17_{2S\text{-}S}$ occurs according to the first-order rate law and half-life of 42 min (Fig. 2B), suggesting that these disulfides are reduced cooperatively and ~3 h incubation is needed to reach the equilibrium.

Midpoint redox potentials for $Cox17_{2S\text{-}S}$/$Cox17_{3S\text{-}S}$ redox pair

In GSH/GSSG redox buffers, the average mass of Cox17 at equilibrium increased at environmental redox potential values below −200 mV, which reflects the shift of equilibrium between $Cox17_{3S\text{-}S}$ and $Cox17_{2S\text{-}S}$ forms and allows calculation of fractional content of $Cox17_{2S\text{-}S}$ form by taking into account $Cox17_{3S\text{-}S}$ and $Cox17_{2S\text{-}S}$ forms. In order to obtain the midpoint redox potential value for $Cox17_{2S\text{-}S}$/$Cox17_{3S\text{-}S}$ couple, the dependence of fractional content of $Cox17_{2S\text{-}S}$ from E_h

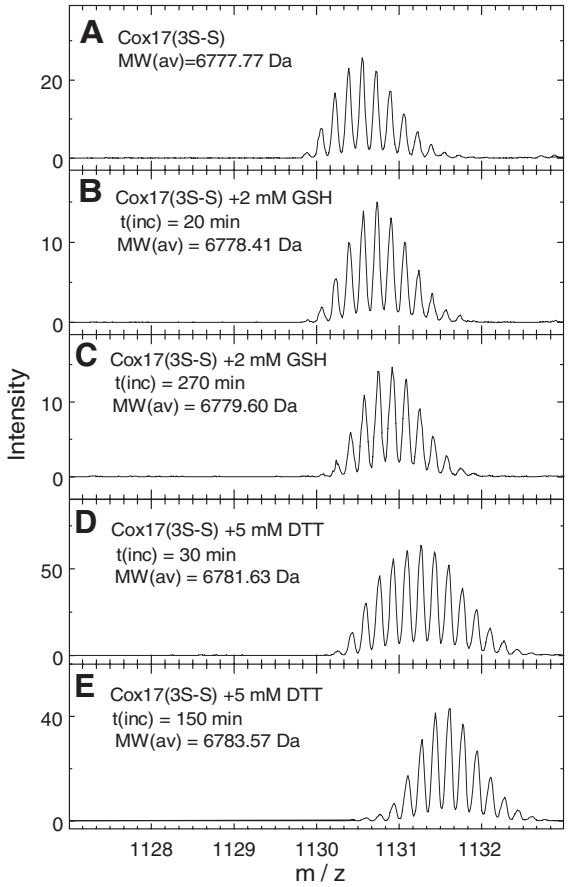

FIG. 1. High resolution ESI MS spectra of Cox17 in the absence and presence of GSH and DTT. Conditions: 5 μM $Cox17_{3S\text{-}S,}$ 20 mM ammonium acetate, pH 7.5; T = 40°C, (**A**) $Cox17_{3S\text{-}S,}$ (**B**) $Cox17_{3S\text{-}S}$ incubated for 20 min with 2 mM GSH; (**C**) $Cox17_{3S\text{-}S}$ incubated for 270 min with 2 mM GSH; (**D**) $Cox17_{3S\text{-}S}$ incubated for 30 min with 5 mM DTT; (**E**) $Cox17_{3S\text{-}S}$ incubated for 150 min with 5 mM DTT. +6 charge states are presented and average molecular masses have been calculated by using Bioanalyst program.

was fitted to equation (4) (Fig. 3A),which yielded a midpoint redox potential equal to $E_{m1} = -227 \pm 0.5$ mV (pH 7.5, 40°C). In addition to the major $Cox17_{3S\text{-}S}$ and $Cox17_{2S\text{-}S}$ forms, the $Cox17_{2S\text{-}S}$-GSH and $Cox17_{2S\text{-}S}$-$(GSH)_2$ adducts were also detected by ESI-MS. The fractional content of these adducts was dependent on the redox potential of the environment as presented in Fig. 3A.

Midpoint redox potential for $Cox17_{2S\text{-}S}$/$Cox17_{3S\text{-}S}$ couple as well as fractional contents of $Cox17_{2S\text{-}S}$-GSH and $Cox17_{2S\text{-}S}$-$(GSH)_2$ adducts were also determined in 5 mM GSH/GSSG redox buffer (Fig. 3B). The calculated midpoint redox potential for $Cox17_{3S\text{-}S}$ /$Cox17_{2S\text{-}S}$ pair was $E_{m1} = -229 \pm 0.8$ mV (pH 7.5, 40°C) that is similar to the E_{m1} value, determined in 1 mM GSH/GSSG redox buffer.

Effect of Zn(II) ions on midpoint redox potential of $Cox17_{2S\text{-}S}$ / $Cox17_{3S\text{-}S}$ pair

The results presented in Fig. 4 demonstrate that the $Cox17_{2S\text{-}S}$/$Cox17_{3S\text{-}S}$ redox equilibrium is affected by Zn(II)

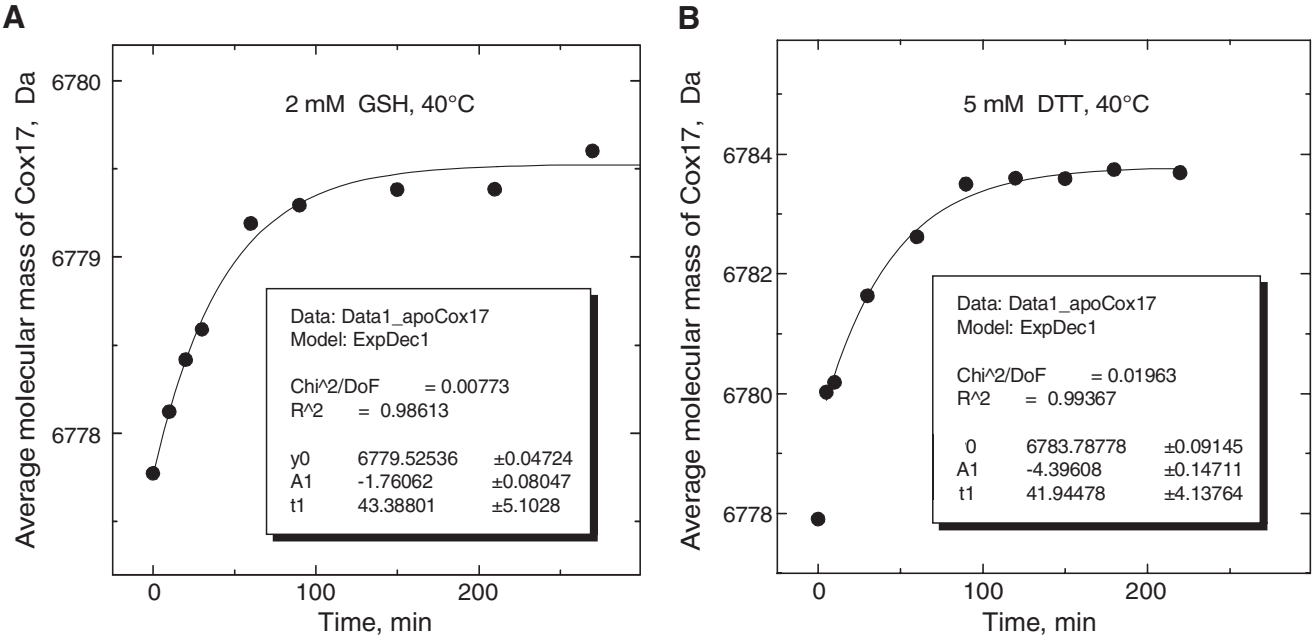

FIG. 2. Kinetics of $Cox17_{3S\text{-}S}$ reduction with GSH and DTT monitored by increase of average molecular weight of Cox17. Conditions: 5 μM $Cox17_{3S\text{-}S}$; 20 mM ammonium acetate, pH 7.5; T = 40°C, (**A**) 2 mM GSH: (**B**) 5 mM DTT. Average molecular masses have been calculated by using Bioanalyst program. *Solid lines*, fitted curves.

ions, which protect Cox17 from oxidation and shift the midpoint redox potential to more positive values: 10 μM Zn(II) shifts E_{m1} by 17 mV, whereas 50 μM Zn(II) shifts E_{m1} by 22 mV in 1 mM GSH/GSSG redox buffer. Besides shifting of E_{m1}, Zn(II) ions also reduced the maximal level of $Cox17_{2S\text{-}S}$-GSH adducts.

The effect of Zn(II) ions on the E_{m1} in 5 mM GSH/GSSG redox buffer presented in Fig. 4B indicates that at higher concentrations of GSH 10 μM Zn(II) shifts E_{m1} by 14 mV, while 50 μM Zn(II) shifts the value of E_{m1} by 26 mV. The Zn(II)-induced shifts in E_{m1} are similar in the 5 mM and in the 1 mM GSH/GSSG buffer.

Reduction $Cox17_{3S\text{-}S}$ with GSH in the presence of millimolar concentrations of Zn(II) ions

The reduction of $Cox17_{3S\text{-}S}$ with GSH did not lead to the formation of fully reduced $Cox17_{0S\text{-}S}$ even after prolonged incubation. However, in the presence of millimolar concentrations of Zn(II) ions, reduction of $Cox17_{3S\text{-}S}$ with 2 mM GSH leads to the formation of fully reduced $Cox17_{0S\text{-}S}$. The process is slow and occurs at 40°C in the presence of 5 and 10 mM Zn(II) with a half-life ~150 min (Fig. 5).

Midpoint redox potentials for $Cox17_{0S\text{-}S}$ / $Cox17_{2S\text{-}S}$ redox pair

Average mass of Cox17 in DTT/DTT_{ox} redox buffers determined after 3 h of incubation at 40°C are presented in Fig. 6. Average mass of $Cox17_{2S\text{-}S}$ at equilibrium increases up to 4 Da at environmental redox potential values below −300 mV, which reflects the equilibrium position between $Cox17_{2S\text{-}S}$ and $Cox17_{0S\text{-}S}$ forms. The midpoint redox potential value for $Cox17_{0S\text{-}S}/Cox17_{2S\text{-}S}$ couple was calculated from the dependence of fractional content of $Cox17_{0S\text{-}S}$ from E_h, presented in Fig. 5. The fitting of data to equation (1) yielded a midpoint redox potential equal to $E_{m2} = -324$ mV (pH 7.5, 40°C).

Effect of Zn(II) ions on midpoint redox potential of $Cox17_{0S\text{-}S}/Cox17_{2S\text{-}S}$ pair

We have also determined the effect of 10 μM Zn(II) ions on $Cox17_{0S\text{-}S}/Cox17_{2S\text{-}S}$ redox equilibrium. Results presented in Fig. 6 demonstrate that 10 μM Zn(II) shifts E_{m2} by 21 mV to more positive values and therefore the effect of 10 μM Zn(II) ions on E_{m2} was more pronounced as its effect on E_{m1}.

Binding of Zn(II) ions to Cox17

$Cox17_{0S\text{-}S}$ and $Cox17_{2S\text{-}S}$, were reconstituted with slight excess of Zn(II) in the presence of DTT, and $ZnCox17_{2S\text{-}S}$ or mainly $Zn_2Cox17_{0S\text{-}S}$ forms were observed in ESI-MS spectra (Fig. 7) similarly to our previous studies (28). In the case of $Zn_1Cox17_{2S\text{-}S}$, the increase in the concentration of DTT resulted in a decrease of $Zn_1Cox17_{2S\text{-}S}$ peak and an increase of the apo-protein peaks (Fig. 7A), indicating that millimolar DTT competes with protein for binding of Zn(II)ions. In the case of $Zn_2Cox17_{0S\text{-}S}$, a two-step demetallation process was observed with the intermediary formation of $Zn_1Cox17_{0S\text{-}S}$ and the final formation of apo-$Cox17_{0S\text{-}S}$ at 35 mM DTT (Figs. 7B and C). Apparent dissociation constants for the Zn_1Protein complexes were calculated according to the following simplified reaction scheme introduced in our previous study for Cu(I) complexes (28):

$$\text{Protein} + \text{Zn(II)} \xleftrightarrow{K_{Zn}} \text{Zn}_1\text{Protein} \quad (5)$$

$$\text{DTT} + \text{Zn(II)} \xleftrightarrow{K_D} \text{Zn}_1\text{DTT} \quad (6)$$

where K_{Zn} is the dissociation constant for the Zn_1Protein complex and K_D is the conditional dissociation constant for

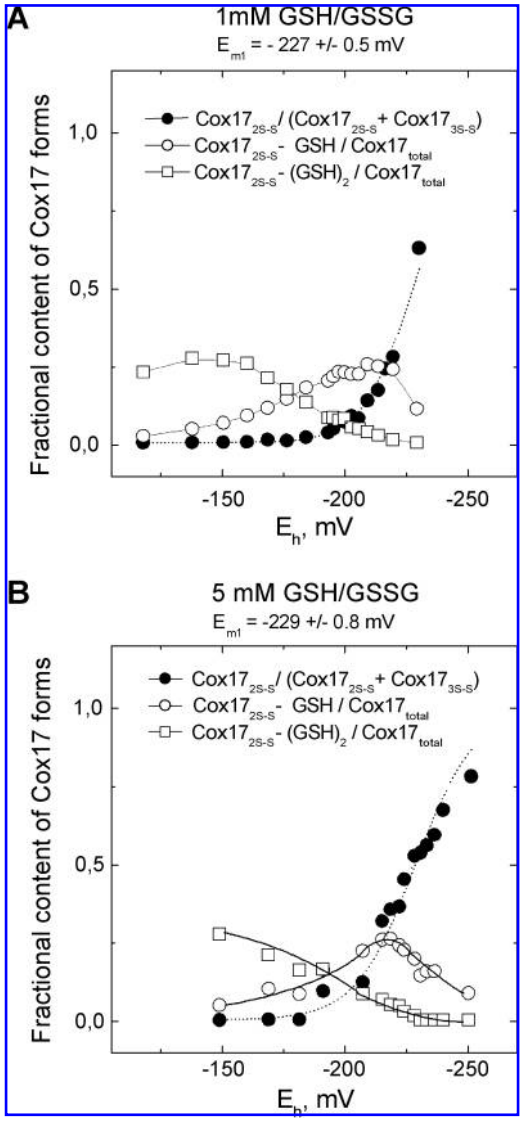

FIG. 3. Determination of redox midpoint potential for $Cox17_{3S\text{-}S} \leftrightarrow Cox17_{2S\text{-}S}$ couple by ESI MS in GSH/GSSG redox buffers. Fractional content of $Cox17_{2S\text{-}S}$ form (-•-) and $Cox17_{2S\text{-}S}$-GSH (-○-), $Cox17_{2S\text{-}S}$-$(GSH)_2$ (-□-) adducts at different environmental redox potential values generated by 1 m*M* GSG/GSSG (**A**) and 5 m*M* GSH/GSSG (**B**) redox buffer. Conditions: 5 μM Cox17; 20 m*M* ammonium acetate, pH 7.5; T = 40°C; incubation time: 3 h. *Solid lines*, fitted curves.

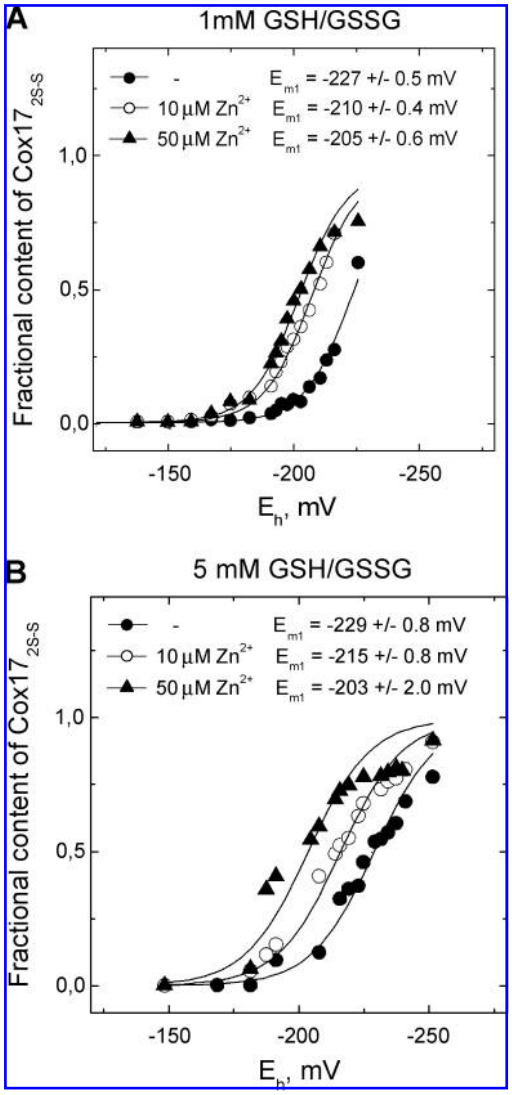

FIG. 4. Effect of Zn(II) ions midpoint redox potential for $Cox17_{3S\text{-}S}/Cox17_{2S\text{-}S}$ couple in GSH/GSSG redox buffer. Fractional content of $Cox17_{2S\text{-}S}$ form in the absence (-•-) and in the presence of 10 μM (-○-) and 50 μM Zn(II) ions (▲) at different environmental redox potential values generated by 1 m*M* GSG/GSSG (**A**) and 5 m*M* GSH/GSSG (**B**) redox buffers. Conditions: 5 μM Cox17; 20 m*M* ammonium acetate, pH 7.5; T = 40°C; incubation time: 3 h. *Solid lines*. fitted curves.

the Zn(II)-DTT complex, which at pH = 7.4, I = 0.1, T = 25°, C is equal to 1.26×10^{-7} *M* (17). Values for K_{Zn} were calculated in two steps: first, by using the K_D value for Zn(II)DTT complex, the concentrations of free Zn(II) ions in the presence of various concentrations of DTT were calculated. Second, fractional content of Zn_1Protein species (Y), calculated from the intensities of apo-$Cox17_{2S\text{-}S}$ and $Zn_1Cox17_{2S\text{-}S}$ peaks, $Zn_2Cox17_{0S\text{-}S}$ and $Zn_1Cox17_{0S\text{-}S}$, as well as for $Zn_1Cox17_{0S\text{-}S}$ and apo-$Cox17_{0S\text{-}S}$ peaks in ESI-MS spectra, $[Y = I_{Zn1Protein}/(I_{Protein} + I_{Zn1Protein})]$, was correlated with the concentration of free Zn(II) ions in the sample. Obtained binding curves for various metallation steps are presented in Fig. 8. The binding isotherms obtained were nonlinearly fitted with a common hyperbolic equation, corresponding to a simple 1:1 binding equilibrium by program Origin 6.1. The following values for the apparent dissociation constants were obtained: $Zn_1Cox17_{2S\text{-}S}$: $K_{Zn} = 0.29 \pm 0.04$ n*M*; $Zn_2Cox17_{0S\text{-}S}$: $K_{Zn} = 0.32 \pm 0.12$ n*M*; $Zn_1Cox17_{0S\text{-}S}$: $K_{Zn} = 0.067 \pm 0.009$ n*M*. In separate ESI-MS experiments we established that GSH competes with $Zn_1Cox17_{2S\text{-}S}$ and $Zn_2Cox17_{0S\text{-}S}$ only at high millimolar concentrations, however, GSH as ionic compound caused substantial decrease of peak intensities in ESI-MS spectra due to ionic suppression.

Discussion

In the current work, we have elaborated a new ESI-TOF MS method for the determination of protein midpoint redox po-

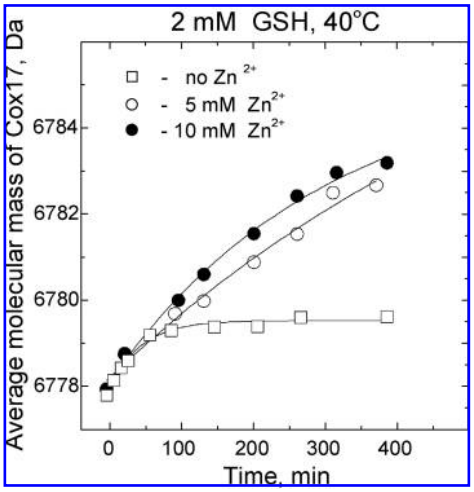

FIG. 5. Kinetics of $Cox17_{3S\text{-}S}$ reduction with GSH in the presence of millimolar concentrations of Zn(II) ions. Conditions: concentration of Zn(II) ions: (-□-) 0 m*M*, (-○-), 5 m*M* (-•-), 10 m*M*; 5 μM Cox17; 20 m*M* ammonium acetate, pH 7.5; T = 40°C. *Solid line*, fitted curve.

tentials in the presence of Zn(II) ions. Results demonstrate that equilibrium between reduced and oxidized (disulfide-containing) forms of the protein could be reliably monitored by the determination of the accurate average molecular weight of the protein mixture at different environmental redox potential values. Direct mass measurement was possible in the case of DTT/DTT_{ox} buffers as DTT does not reduce the

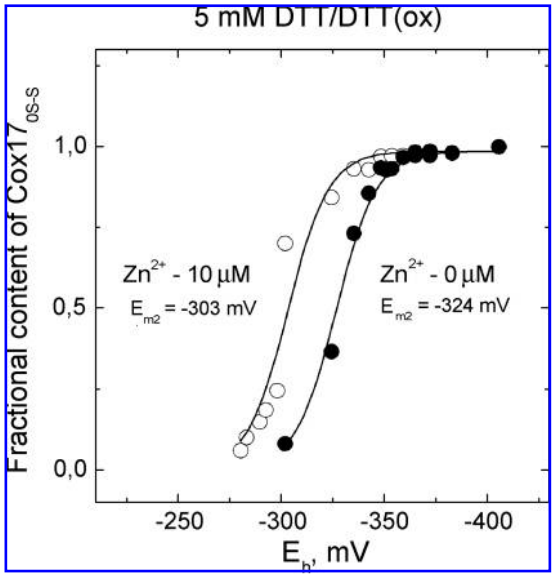

FIG. 6. Effect of Zn(II) ions on $Cox17_{0S\text{-}S} \leftrightarrow Cox17_{0S\text{-}S}$ redox equilibrium. Fractional content of $Cox17_{0S\text{-}S}$ form in the absence (-•-) and in the presence of 10 μM Zn(II) ions at different environmental redox potential values generated by 5 m*M* DTT/DTTox redox buffer. Conditions: 5 μM Cox17; 20 m*M* ammonium acetate, pH 7.5; T = 40°C; incubation time: 3 h. *Solid lines*, fitted curves.

efficiency of the ionization of protein in the electrospray ionization process. The biological redox compound GSH is an ionic substance that reduces the efficiency of the ionization of the protein at millimolar concentrations and therefore its removal by desalting was necessary before MS measurements. The mass accuracy of the QSTAR Elite ESI-TOF MS instrument allowed the determination of molecular mass of Cox17 with accuracy of 0.02 Da, which is sufficient for precise monitoring the reduction of one disulfide bond (mass difference of 2 Da). The elaborated approach is also applicable for investigation of other biological redox switches and redox sensors in the presence of metal ions.

The new ESI-TOF MS based method yielded slightly different E_m values ($E_{m1} = 227$ mV and $E_{m2} = 324$ mV, pH 7.5, 40°C) as compared to those determined by another approach, where trapping of free SH groups by alkylation and subsequent separation of different redox forms by HPLC or MALDI-TOF MS analysis was used ($E_{m1} = 198$ mV and $E_{m2} = 340$ mV, pH 7.6, 37°C) (40). Since the additional trapping and separation steps might each introduce errors in the range of 10 mV (16) we suggest that the new E_m values are more correct. Besides the direct estimation of equilibrium ratios of the fully reduced and the oxidized forms of the protein, the ESI MS-based method also allows the quantitative determination of protein-GSH adducts that might be generated at certain redox potential values in GSH/GSSG redox buffers. The present results confirm earlier findings that the contents of $Cox17_{2S\text{-}S}$-GSH and $Cox17_{2S\text{-}S}$-2GSH adducts depend on the redox potential of the environment. The content of $Cox17_{2S\text{-}S}$-GSH forms a bell-shaped curve with a maximum level of 25% around the midpoint redox potential E_{m1} in both 1 and 5 m*M* GSH/GSSG redox buffers, indicating that the content of the glutathionylated forms of Cox17 depends on the environmental redox potential value and does not depend on the molar excess of GSH over Cox17. Similar conclusions could be also drawn for the doubly glutathionylated Cox17 form, $Cox17_{2S\text{-}S}$-2GSH, which level reached maximum at E_h values below −150 mV in the case of 1 and 5 m*M* GSH/GSSG redox buffers. The occurrence of mixed disulfides of Cox17 with GSH might play a regulatory role in the functioning of Cox17, as suggested before (40).

The equilibrium between $Cox17_{2S\text{-}S}$ and $Cox17_{0S\text{-}S}$ was studied in DTT/DTT_{ox} buffers. As only a single redox transition resulting in a mass increase by 4 Da was observed for this equilibrium, we can conclude that the reduction of two disulfides in $Cox17_{2S\text{-}S}$ occurs cooperatively. Most probably the S–S bridge between Cys^{25} and Cys^{54} in the structure of apo$Cox17_{2S\text{-}S}$ (Fig. 9) (2) is reduced first, which leads to the opening of the protein structure, where the another S–S bond between Cys^{35} and Cys^{44} is easily accessible from the solution and can be quickly reduced by DTT.

Determination of the protein midpoint redox potentials in the presence of Zn(II) ions

The major advantage of the elaborated ESI MS-based method is its direct applicability for accurate determination of the effect of metal ions on the protein redox equilibria. The obtained results demonstrate that 10 μM Zn(II) ions shifts E_{m1} by 17 and 14 mV in 1 and 5 m*M* GSH/GSSG redox buffers accordingly, whereas 50 μM Zn(II) shifted E_{m1} by 22 and 26 mV in 1 and 5 m*M* GSH/GSSG redox buffers. This allows

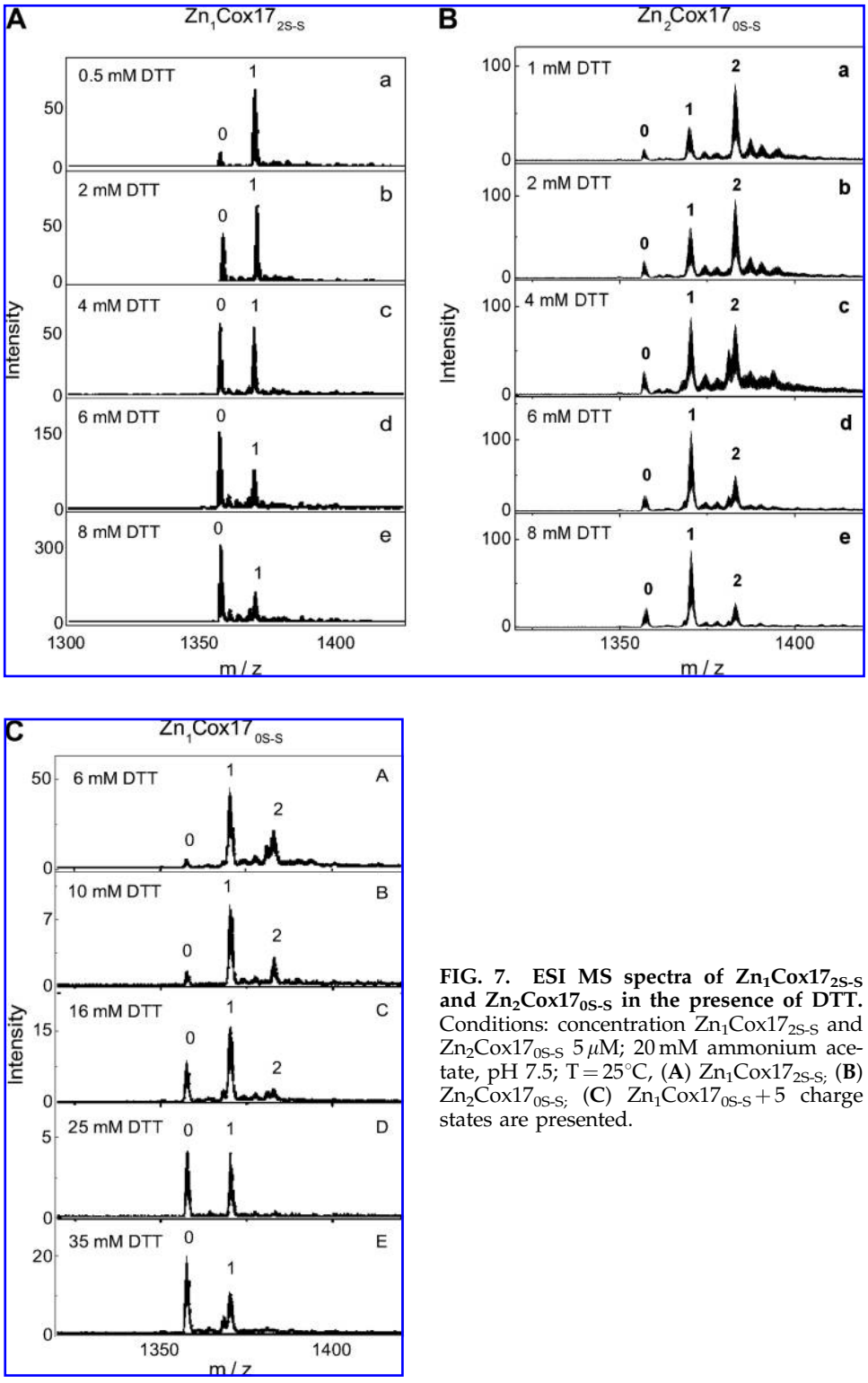

FIG. 7. ESI MS spectra of $Zn_1Cox17_{2S\text{-}S}$ and $Zn_2Cox17_{0S\text{-}S}$ in the presence of DTT. Conditions: concentration $Zn_1Cox17_{2S\text{-}S}$ and $Zn_2Cox17_{0S\text{-}S}$ 5 μM; 20 mM ammonium acetate, pH 7.5; T = 25°C, (**A**) $Zn_1Cox17_{2S\text{-}S;}$ (**B**) $Zn_2Cox17_{0S\text{-}S;}$ (**C**) $Zn_1Cox17_{0S\text{-}S}$ + 5 charge states are presented.

us to draw two conclusions: First: the effect of Zn(II) ions does not depend on concentration of GSH. Consequently the effect of Zn(II) ions is dependent on protein–metal interaction and GSH does not compete with $Cox17_{2S\text{-}S}$ for binding of Zn(II) ions at concentrations used. Second, the effect of Zn(II) ions on E_{m1} is more pronounced at increased concentrations of Zn(II) ions, which indicates that metal-induced modulation of redox properties depends on metal concentration. We also tested the effect of higher millimolar concentrations of Zn(II) on the reduction of $Cox17_{3S\text{-}S}$ with 2 m*M* GSH. Surprisingly, millimolar Zn(II) promoted the slow formation of a fully reduced $Cox17_{0S\text{-}S}$ in the presence of 2 mM GSH (Fig. 6), which suggests that the effect of Zn(II) ions on E_{m1} is not saturated at high micromolar metal concentrations and at millimolar concentrations Zn(II) ions have also pronounced effect on the redox equilibrium between $Cox17_{2S\text{-}S}$ and $Cox17_{0S\text{-}S}$.

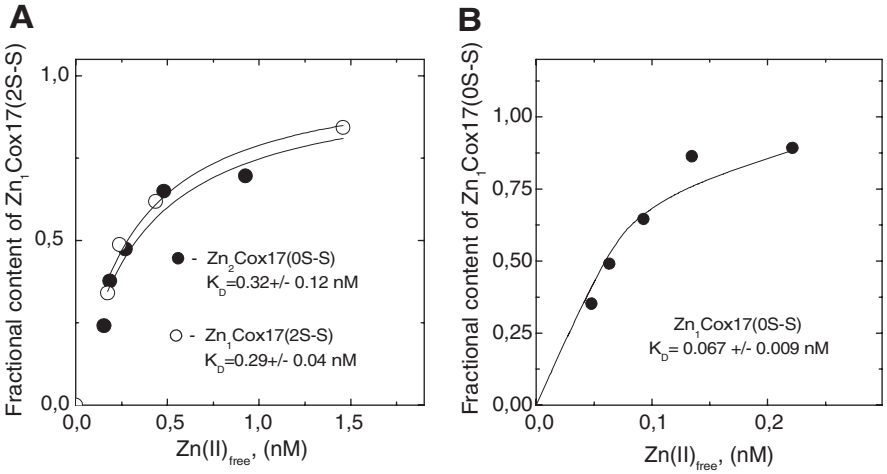

FIG. 8. Determination of the apparent dissociation constants for $Zn_1Cox17_{2S\text{-}S}$, $Zn_2Cox17_{0S\text{-}S}$ and $Zn_2Cox17_{0S\text{-}S}$ complexes. Dependence of the fractional content of metallated Cox17 forms ($Y = I_{ZnCox17}/(I_{Cox17} + I_{ZnCox17})$ from the concentration of free Zn(II) ions in metal competition experiment. (20 m*M* ammonium acetate pH 7.5, 25°C) *Solid line* shows the fitted curve for hyperbola with $K_{Zn} = 0.29 \times 10^{-9}$ *M* ($Zn_1Cox17_{2S\text{-}S}$). $K_{Zn} = 0.32 \times 10^{-9}$ *M* ($Zn_2Cox17_{2S\text{-}S}$), and $K_{Zn} = 0.067 \times 10^{-9}$ *M* ($Zn_1Cox17_{2S\text{-}S}$).

Zn(II) ions also had an effect on the midpoint redox potential of $Cox17_{0S\text{-}S}/Cox17_{2S\text{-}S}$ couple, determined by using DTT/DTT_{ox} redox buffers and this effect was more pronounced than the effect of Zn(II) ions on the E_{m1}. 10 μM Zn(II) increased the E_{m2} value two times more than the E_{m1} value. The stronger effect of Zn(II) ions on E_{m2} suggests that binding of Zn(II) ions to the fully reduced $Cox17_{0S\text{-}S}$ is stronger as compared with $Cox17_{2S\text{-}S}$. Indeed, Zn(II)-binding affinities for different Cox17 forms, determined in the current study indicate that the apparent dissociation constant for $Zn_2Cox17_{0S\text{-}S}$ complex, $K_{Zn} = 0.067$ n*M*, is 5 times lower than that for $Zn_1Cox17_{2S\text{-}S}$ ($K_{Zn} = 0.29$ n*M*). Moreover, even 2 m*M* GSH did not demetallate $Zn_2Cox17_{0S\text{-}S}$, which indicates that $Cox17_{0S\text{-}S}$ can effectively compete for Zn(II) ions with millimolar GSH in cellular conditions.

Biological context

Cox17 fulfils its primary biological role as a copper chaperone for CCO in IMS. Cox17 and other proteins containing twin Cys-X_9-Cys motifs (Mia 40, Cox19, Cox23) or twin Cys-X_3-Cys motifs (small Tim proteins) are transported into IMS by a special oxidative mechanism (13). According to this mechanism, fully reduced proteins enter IMS through mitochondrial outer membrane pores. In IMS, the twin Cys-X_9-Cys motif is oxidized with the involvement of Mia40 proteins and functions as a thiol-based redox switch (26). The oxidation leads to the formation of coiled coil helix–coiled coil helix structural motif (CHCH), where two short helixes are connected with two interhelical disulfide bonds (Fig. 9) and oxidative folding is crucial for retention of these proteins in IMS. In the case of Cox17, the partially oxidized $Cox17_{2S\text{-}S}$ is also biologically active and participates in the metallation of Sco1 protein (2, 3). However, in cellular conditions it is crucial to keep *de novo* synthesized cytoplasmic Cox17 in fully reduced state until it is transported into IMS.

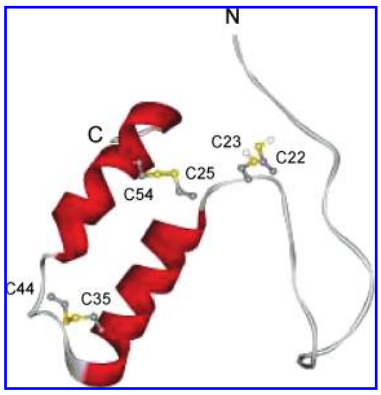

FIG. 9. Solution structure of human apo-$Cox17_{2S\text{-}S}$. One structure from 2RN9 (2) is presented, where the first 17 amino acids are unstructured, disulfide bridges C^{25}–C^{54} and C^{35}–C^{44} as well as C^{22} and C^{23} are displayed. (For interpretation of the references to color in this figure legend, the reader is referred to the web version of this article at www.liebertonline.com/ars).

A major factor determining the position of biological redox switches under normal cellular conditions is the redox potential in the local cellular compartment. The determination of the redox potential in cellular cytosol as well as in different cellular compartments is an active field of research. This is a complicated task since the total cellular redox potential is composed of different redox systems that, however, might not be always in equilibrium with cellular redox buffer (16). By this reason, the application of different redox couples for the determination of the cellular redox potential might yield different values. For instance, the redox potential values in eukaryotic cytosol determined from analytical concentrations of GSH and GSSG vary in a broad range from −200 to −290 mV (pH 7.0), whereas the latter value corresponds to normal conditions (16, 22, 27). Similar cellular redox potential value −280 mV (pH 7.0) has been determined from the cellular equilibrium between reduced and oxidized thioredoxin-1 (16, 38). However, redox potential values determined *in situ* by using different fluorescent redox sensor proteins are more negative (more reducing) and lay in the range from −280 to −320 mV (pH 7.0) (4, 12, 22).

Discrepancy between the listed cellular redox potential values determined might arise from the methods used, however, it is also possible that redox sensor systems used might not be in equilibrium with cellular redox buffers. Moreover, our current results indicate that Zn(II) ions shift redox equilibria of thiol-based redox switches and it is not excluded that redox equilibria of thiol-based redox couples used for determination of cellular redox potential might also be influenced by Zn(II) ions, because the total cellular concentration is as high as 250 μM (18) and a substantial part of it is bound into

labile complexes (27). If the further studies confirm that cellular Zn(II) ions have significant influence on the redox equilibria of redox sensors and thioredoxins, then the methodology for determination of cellular redox potential has to be critically revised and improved.

The midpoint redox potential of $Cox17_{0SS}/Cox17_{2SS}$ couple (E_{m2}) is at pH 7.5 around −324 mV (at pH 7.0 $E_{m2} = -294$ mV), which is close to the cellular redox potential E = −286 mV (pH 7.0) (14). In such conditions, Cox17 shall be 65% oxidized to $Cox17_{2SS}$ (as estimated from Fig. 6). However, $Cox17_{2SS}$ cannot enter into IMS and additional factors should be involved in the stabilization of $Cox17_{0S\text{-}S}$ in the cytosol. In the case of Tim10 protein that contains twin Cys-X_3-Cys motif and uses oxidative mechanism for transport into IMS; it has been suggested that binding of Zn(II) ions inhibits protein oxidation and facilitates kinetically its transport into IMS (23). We demonstrated for the first time that Zn(II) ions present at low micromolar levels can substantially shift the protein midpoint redox potential of $Cox17_{0S\text{-}S}/Cox17_{2S\text{-}S}$ couple to more positive values and therefore protect $Cox17_{0S\text{-}S}$ by thermodynamic reasons from oxidation in the cytoplasm. 10 μM Zn(II) increased the E_{m2} value by 21 mV and shifts E_{m2} value to 271 mV (pH 7.0). It can be estimated from Fig. 6 that 21 mV shift in E_{m2} keeps 80 % of the total Cox17 in the fully reduced state. At the higher concentrations of Zn(II) ions, the protection of Cox17 from oxidation is almost complete. $Cox17_{0S\text{-}S}$ can bind two Zn(II) ions (28) and the apparent dissociation constants for $Zn_2Cox17_{0S\text{-}S}$ and $Zn_1Cox17_{0S\text{-}S}$ complexes, determined in the current study, are 0.32 and 0.067 nM, respectively. Cellular zinc exists in three pools: a stabile protein-bound pool, a metallothionein-bound pool, and a labile zinc pool, whereas the latter consists mainly from Zn(II)-GSH complex (30). Our results demonstrate that $Cox17_{0S\text{-}S}$ can effectively compete with high millimolar DTT and GSH for Zn(II) binding, which indicates that $Cox17_{0S\text{-}S}$ might be metallated by Zn(II) ions in cellular conditions.

After transport into IMS, fully reduced Cox17 is oxidized to $Cox17_{2S\text{-}S.}$ This reaction is catalyzed by Mia 40 proteins (5). However, oxidation should also be thermodynamically favorable. The redox potential value in IMS, determined by ratio of GSH/GSSG couple is equal to −255 mV, (pH 7.0) (14), which is more positive (oxidative) as that in the cytoplasm (E = −286 mV, pH 7.0) (14). Redox potential in IMS shifts $Cox17_{0SS} \leftrightarrow Cox17_{2SS}$ equilibrium towards $Cox17_{2SS}$ state, which is the functional state of protein in IMS (1).

The second oxidative switch converts $Cox17_{2S\text{-}S}$ to the fully oxidized protein $Cox17_{3S\text{-}S}$, which can not bind metals (28, 40). Midpoint redox potential of this switch is equal to −226 mV (pH 7.5, 40°C), which is much more positive than cellular redox potential values under normal conditions. However, the cellular redox potential is known to increase up to 80 mV in oxidative conditions (16, 38) where $Cox17_{2S\text{-}S}$ could also be partially oxidized to $Cox17_{3S\text{-}S}$. Our results demonstrate that Zn(II) ions can protect $Cox17_{2S\text{-}S}$ from undesirable oxidation, which might occur in IMS as well as in the cytoplasm by influence of oxidative stimuli. Such a protection might avoid the inactivation of $Cox17_{2S\text{-}S}$ and promote its functioning in IMS.

Acknowledgments

This work was supported by Estonian Science Foundation project 7191. Ms. K. Zovo thanks the World Federation of Scientists for support. We thank Ms. Niina Sokolova for technical assistance in protein expression and ESI MS experiments.

Abbreviations

Cox17, cytochrome-c oxidase copper chaperone; CCO, cytochrome-c oxidase, DTT, dithiothreitol; GSH, glutathione; GSSG, oxidized gluthathione; IMS, mitochondrial intermembrane space.

Disclosure Statement

No competing financial interests exist.

References

1. Banci L, Bertini I, Ciofi-Baffoni S, Hadjiloi T, Martinelli M, and Palumaa P. Mitochondrial copper(I) transfer from Cox17 to Sco1 is coupled to electron transfer. *Proc Natl Acad Sci USA* 105: 6803–6808, 2008.
2. Banci L, Bertini I, Ciofi–Baffoni S, Janicka A, Martinelli M, Kozlowski H, and Palumaa P. A structural-dynamical characterization of human Cox17. *J Biol Chem* 283: 7912–7920, 2008.
3. Banci L, Bertini I, Ciofi-Baffoni S, Leontari I, Martinelli M, Palumaa P, Sillard R, and Wang S. Human Sco1 functional studies and pathological implications of the P174L mutant. *Proc Natl Acad Sci USA* 104: 15–20, 2007.
4. Bjornberg O, Ostergaard H, and Winther JR. Measuring intracellular redox conditions using GFP-based sensors. *Antioxid Redox Signal* 8: 354–361, 2006.
5. Chacinska A, Pfannschmidt S, Wiedemann N, Kozjak V, Sanjuan Szklarz LK, Schulze–Specking A, Truscott KN, Guiard B, Meisinger C, and Pfanner N. Essential role of Mia40 in import and assembly of mitochondrial intermembrane space proteins. *EMBO J* 23: 3735–3746, 2004.
6. Cleland WW. Dithiothreitol, a new protective reagent for SH groups. *Biochemistry* 3: 480–482, 1964.
7. Dalle–Donne I, Rossi R, Giustarini D, Colombo R, and Milzani A. S-glutathionylation in protein redox regulation. *Free Radic Biol Med* 43: 883–898, 2007.
8. Dutton PL. Redox potentiometry: determination of midpoint potentials of oxidation- reduction components of biological electron-transfer systems. *Methods Enzymol* 54: 411–435, 1978.
9. Fratelli M, Demol H, Puype M, Casagrande S, Eberini I, Salmona M, Bonetto V, Mengozzi M, Duffieux F, Miclet E, Bachi A, Vandekerckhove J, Gianazza E, and Ghezzi P. Identification by redox proteomics of glutathionylated proteins in oxidatively stressed human T lymphocytes. *Proc Natl Acad Sci USA* 99: 3505–3510, 2002.
10. Ghezzi P, Bonetto V, and Fratelli M. Thiol-disulfide balance: From the concept of oxidative stress to that of redox regulation. *Antioxid Redox Signal* 7: 964–972, 2005.
11. Glerum DM, Shtanko A, and Tzagoloff A. Characterization of COX17, a yeast gene involved in copper metabolism and assembly of cytochrome oxidase. *J Biol Chem* 271: 14504–11459, 1996.
12. Hanson GT, Aggeler R, Oglesbee D, Cannon M, Capaldi RA, Tsien RY, and Remington SJ. Investigating mitochondrial redox potential with redox-sensitive green fluorescent protein indicators. *J Biol Chem* 279: 13044–13053, 2004.
13. Herrmann JM and Kohl R. Catch me if you can! Oxidative protein trapping in the intermembrane space of mitochondria. *J Cell Biol* 176: 559–563, 2007.

14. Hu J, Dong L, and Outten CE. The redox environment in the mitochondrial intermembrane space is maintained separately from the cytosol and matrix. *J Biol Chem* 283: 29126–29134, 2008.
15. Jiang K, Schwarzer C, Lally E, Zhang S, Ruzin S, Machen T, Remington SJ, and Feldman L. Expression and characterization of a redox-sensing green fluorescent protein (reduction-oxidation-sensitive green fluorescent protein) in Arabidopsis. *Plant Physiol* 141: 397–403, 2006.
16. Kemp M, Go YM, and Jones DP. Nonequilibrium thermodynamics of thiol/disulfide redox systems: a perspective on redox systems biology. *Free Radic Biol Med* 44: 921–937, 2008.
17. Krezel A, Lesniak W, Jezowska–Bojczuk M, Mlynarz P, Brasun J, Kozlowski H, and Bal W. Coordination of heavy metals by dithiothreitol, a commonly used thiol group protectant. *J Inorg Biochem* 84: 77–88, 2001.
18. Krezel A and Maret W. Zinc-buffering capacity of a eukaryotic cell at physiological pZn. *J Biol Inorg Chem* 11: 1049–1062, 2006.
19. Kröncke KD. Zinc finger proteins as molecular targets for nitric oxide-mediated gene regulation. *Antioxid Redox Signal* 3: 565–575, 2001.
20. Leichert LI and Jakob U. Protein thiol modifications visualized *in vivo*. *PLoS Biol* 2: 1723–1737, 2004.
21. Linke K and Jakob U. Not every disulfide lasts forever: disulfide bond formation as a redox switch. *Antioxid Redox Signal* 5: 425–434, 2003.
22. Lopez–Mirabal HR and Winther JR. Redox characteristics of the eukaryotic cytosol. *Biochim Biophys Acta* 1783: 629–640, 2008.
23. Lu H and Woodburn J. Zinc binding stabilizes mitochondrial Tim10 in a reduced and import-competent state kinetically. *J Mol Biol* 353: 897–910, 2005.
24. Maret W. Zinc coordination environments in proteins as redox sensors and signal transducers. *Antioxid Redox Signal* 8: 1419–1441, 2006.
25. Marri L, Trost P, Trivelli X, Gonnelli L, Pupillo P, and Sparla F. Spontaneous assembly of photosynthetic supramolecular complexes as mediated by the intrinsically unstructured protein CP12. *J Biol Chem* 283: 1831–1838, 2008.
26. Mesecke N, Terziyska N, Kozany C, Baumann F, Neupert W, Hell K, and Herrmann JM. A disulfide relay system in the intermembrane space of mitochondria that mediates protein import. *Cell* 121: 1059–1069, 2005.
27. Ostergaard H, Tachibana C, and Winther JR. Monitoring disulfide bond formation in the eukaryotic cytosol. *J Cell Biol* 166: 337–345, 2004.
28. Palumaa P, Kangur L, Voronova A, and Sillard R. Metal-binding mechanism of Cox17, a copper chaperone for cytochrome c oxidase. *Biochem J* 382: 307–314, 2004.
29. Piotukh K, Kosslick D, Zimmermann J, Krause E, and Freund C. Reversible disulfide bond formation of intracellular proteins probed by NMR spectroscopy. *Free Radic Biol Med* 43: 1263–1270, 2007.
30. Rana U, Kothinti R, Meeusen J, Tabatabai NM, Krezoski S, and Petering DH. Zinc binding ligands and cellular zinc trafficking: apo-metallothionein, glutathione, TPEN, proteomic zinc, and Zn-Sp1. *J Inorg Biochem* 102: 489–499, 2008.
31. Schafer FQ and Buettner GR. Redox environment of the cell as viewed through the redox state of the glutathione disulfide/glutathione couple. *Free Radic Biol Med* 30: 1191–1212, 2001.
32. Smirnova J, Zhukova L, Witkiewicz–Kucharczyk A, Kopera E, Oledzki J, Wyslouch–Cieszynska A, Palumaa P, Hartwig A, and Bal W. Quantitative electrospray ionization mass spectrometry of zinc finger oxidation: the reaction of XPA zinc finger with H(2)O(2). *Anal Biochem* 369: 226–231, 2007.
33. Szajewski RP and Whitesides GM. Rate constants and equilibrium constants for thiol-disulfide interchange reactions involving oxidized glutathione. *J Am Chem Soc* 102: 2011–2016, 1980.
34. Takahashi Y, Kako K, Kashiwabara S, Takehara A, Inada Y, Arai H, Nakada K, Kodama H, Hayashi J, Baba T, and Munekata E. Mammalian copper chaperone Cox17p has an essential role in activation of cytochrome C oxidase and embryonic development. *Mol Cell Biol* 22: 7614–7621, 2002.
35. Trachootham D, Lu W, Ogasawara MA, Nilsa RD, and Huang P. Redox regulation of cell survival. *Antioxid Redox Signal* 10: 1343–1374, 2008.
36. Wang G, Strang C, Pfaffinger PJ, and Covarrubias M. Zn2+-dependent redox switch in the intracellular T1-T1 interface of a Kv channel. *J Biol Chem* 282: 13637–14647, 2007.
37. Wang W, Winther JR, and Thorpe C. Erv2p: characterization of the redox behavior of a yeast sulfhydryl oxidase. *Biochemistry* 46: 3246–3254, 2007.
38. Watson WH and Jones DP. Oxidation of nuclear thioredoxin during oxidative stress. *FEBS Lett* 543: 144–147, 2003.
39. Voronova A, Kazantseva J, Tuuling M, Sokolova N, Sillard R, and Palumaa P. Cox17, a copper chaperone for cytochrome c oxidase: expression, purification, and formation of mixed disulfide adducts with thiol reagents. *Protein Expr Purif* 53: 138–144, 2007.
40. Voronova A, Meyer–Klaucke W, Meyer T, Rompel A, Krebs B, Kazantseva J, Sillard R, and Palumaa P. Oxidative switches in functioning of mammalian copper chaperone Cox17. *Biochem J* 408: 139–148, 2007.

Address reprint requests to:
Peep Palumaa
Akadeemia tee 15
12618 Tallinn, Estonia

E-mail: peepp@staff.ttu.ee

Date of first submission to ARS Central, August 25, 2008; date of final revised submission, November 18, 2008; date of acceptance, November 18, 2008.

This article has been cited by:

1. Julia Smirnova, Jekaterina Muhhina, Vello Tõugu, Peep Palumaa. 2012. Redox and Metal Ion Binding Properties of Human Insulin-like Growth Factor 1 Determined by Electrospray Ionization Mass Spectrometry. *Biochemistry* **51**:29, 5851-5859. [CrossRef]
2. 2009. Current literature in mass spectrometry. *Journal of Mass Spectrometry* **44**:10, 1542-1553. [CrossRef]